Bioorganic Chemistry 36 (2008) 271–277

Contents lists available at ScienceDirect

Bioorganic Chemistry

journal homepage: www.elsevier.com/locate/bioorg

Characterization of two adenosine analogs as fluorescence probes in RNA

Ying Zhao [a], Joseph L. Knee [a,*], Anne M. Baranger [a,b,*]

[a] Department of Chemistry, Wesleyan University, Middletown, CT 06459, USA
[b] Department of Chemistry, University of Illinois at Urbana-Champaign, 600 S. Mathews Avenue, Urbana, IL 61801, USA

ARTICLE INFO

Article history:
Received 30 April 2008
Available online 15 August 2008

Keywords:
RNA
Fluorescence lifetime
Adenosine
Fluorophore
Fluorescence anisotropy

ABSTRACT

The fluorescence properties of two adenosine analogs, 2-(3-phenylpropyl)adenosine [A-3CPh] and 2-(4-phenylbutyl)adenosine [A-4CPh], are reported. As monomers, the quantum yields and the mean lifetimes are 0.011 and 6.22 ns for A-3CPh and 0.007 and 7.13 ns for A-4CPh, respectively. Surprisingly, the quantum yields of the two probes are enhanced 11- to 82-fold upon incorporation into RNA, while the mean lifetimes decrease 23–40%. The data suggest that a subpopulation of molecules is responsible for the fluorescence characteristics and that the distribution of emitting and non-emitting structures is altered upon incorporation of the probes into RNA. Thus, although both adenosine analogs have low quantum yields as monomers, their fluorescence signals are significantly enhanced in RNA. Thermodenaturation experiments and CD spectroscopy indicate that incorporation of the adenosine analogs into three different RNAs does not alter their global structure or stability. Therefore, these probes should be useful for probing events occurring close to the site of modification.

1. Introduction

Fluorescence spectroscopy is one of the most widely used spectroscopic techniques in the fields of biochemistry and molecular biophysics because of its inherent sensitivity and ability to monitor changes in the structural and dynamic properties of biological molecules [1]. Using fluorescence methods to study nucleic acids is a challenge because the bases are only slightly fluorescent. In many cases highly fluorescent probes are attached to the nucleic acids for use in fluorescence assays. Most of the commonly used fluorescent probes, such as fluorescein and rhodamine, have large aromatic ring systems and are attached to the nucleic acids through flexible carbon linkers. As a result, these probes are often less sensitive to structural and environmental changes of the nucleic acids than if the probe is placed directly at the site of interest. Using fluorophores that are chemical analogs of the nucleosides can solve this problem. However, only a limited number of fluorophores that are nucleoside base analogs are available [2–5]. Most of these base analogs are deoxyribonucleosides and are used in DNA fluorescence studies. Only a few base analog fluorophores have been reported that are ribonucleoside analogs [6–10]. The recognition of the importance of RNA in basic biological processes, such as gene expression, has led to a growing need for ribonucleoside base analog fluorophores.

In this paper, we describe the fluorescence properties of two adenosine analogs (A-3CPh and A-4CPh) that were synthesized and utilized in the binding studies of the U1A protein and U1 snRNA described previously [11]. We have incorporated these probes into three different non-duplex structures and have found that these analogs do not alter the global structure or stability of the RNAs. Because the hydrogen bonding functional groups of adenosines are not disturbed in these analogs, these probes should be accommodated into other types of RNA structures with minimal structural perturbation. Surprisingly, although these probes have weak quantum yields as monomers, the quantum yields are enhanced when they are incorporated into RNA.

2. Materials and methods

2.1. Sample preparation

Synthesis of A-3CPh and A-4CPh, incorporation of these probes into RNA, and RNA purification were reported previously [11]. The identity and purity of the free probes were confirmed by NMR spectroscopy and high resolution mass spectrometry. The identity of the RNA was confirmed by MALDI mass spectrometry. Correct incorporation of the nucleotides into RNA sequences was confirmed by HPLC analysis of enzymatic digestion reactions. All RNA solutions were prepared in TE buffer (10 mM Tris–HCl, pH

* Corresponding authors. Fax: +1 860 685 2211 (J.L. Knee), +1 217 244 8024 (A.M. Baranger).
E-mail addresses: jknee@wesleyan.edu (J.L. Knee), baranger@uiuc.edu (A.M. Baranger).

0045-2068/$ - see front matter © 2008 Elsevier Inc. All rights reserved.
doi:10.1016/j.bioorg.2008.06.003

7.4, 1 mM EDTA). The concentrations of RNA solutions were determined by UV absorption at 260 nm.

2.2. Steady-state fluorescence

Steady-state fluorescence spectra were recorded on a Fluoro-Max-2 spectrometer (Jobin Yvon-SPEX division, Instruments S.A., Inc. Metuchen, NJ) equipped with a 150 W xenon lamp and modified Czerny-Turner spectrometers in both the excitation and emission position utilizing Datamax Spectroscopy Software (Galactic Industries, Salem, N.H.). Fluorescence was measured at a 90° angle in an L-format. The fluorimeter was interfaced with a Neslab RTE-111 temperature controller (Thermo Electron Co.) with a remote sensor. Small sample volumes (about 200 μl) were attained using 3×3 mm quartz cuvettes supported by custom built adapters. The excitation and emission slits were set at 0.94 mm to give a 4 nm band-pass. All fluorescence scans were recorded using S/R signal, 1 nm wavelength increments, and a 1-s integration time.

2.3. Quantum yield measurements

A solution of 59.81 nM quinine sulfate in 0.1 N H_2SO_4 was used as a quantum yield standard. The fluorescence emission spectra were processed using GRAMS/AI (version 7) spectroscopy data processing software (Thermo Galactic). UV absorbance of monomer solutions and RNA solutions were measured using a Shimadzu UV-1400 UV/vis absorption spectrometer (Shimadzu Co.).

The quantum yield of the test sample can be calculated using Eq. (1) [12].

$$Q_x = Q_s\left(\frac{B_s}{B_x}\right)\left(\frac{I(\lambda_s)}{I(\lambda_x)}\right)\left(\frac{n_x^2}{n_s^2}\right)\left(\frac{D_x}{D_s}\right) = Q_s\left(\frac{A_s(\lambda_s)}{A_x(\lambda_x)}\right)\left(\frac{I(\lambda_s)}{I(\lambda_x)}\right)\left(\frac{n_x^2}{n_s^2}\right)\left(\frac{D_x}{D_s}\right) \quad (1)$$

where B is the fraction of incident light absorbed, I(λ) is the relative intensity of the exciting light at wavelength λ, n is the average refractive index of the solution, D is the integrated area under the corrected emission spectrum, and $A(\lambda)$ is the absorbance of the solution at the excitation wavelength λ. The subscript s refers to the standard and the subscript x refers to the test sample. If the standard and the sample are dissolved in the same solvent, the average refractive indexes of these two solutions are comparable. When the same excitation wavelength is used, the ratio of the exciting light intensities is one. Thus, Eq. (1) can be simplified to Eq. (2).

$$Q_x = Q_s\left(\frac{A_s(\lambda_s)}{A_x(\lambda_x)}\right)\left(\frac{D_x}{D_s}\right) \quad (2)$$

Eq. (2) has been used to calculate the quantum yields of the A-3CPh and A-4CPh molecules by comparison to quinine sulfate.

Determination of the quantum yields of the probes in RNA is complicated by the overlap of the absorption of other bases in the oligomers with that of the probes. However, if the molar absorption coefficient (ε) of the probe in RNA is similar to that of the free probe, then the quantum yields of the RNA can be determined by using the free probe as the reference compound. It is likely that there is some change in ε upon incorporation of the probe into RNA. Although this change is probably small compared to the changes in quantum yield observed, it is important to keep in mind that this approximation will result in an over- or underestimate of the quantum yield of the probe in the RNA. Because the absorbance of a dilute solute follows Beer's law, the ratio of the absorbance in Eq. (2) can be expressed as the ratio of the concentrations (Eq. (3)) when the molar absorption (ε) of two samples are comparable.

$$Q_x = Q_s\left(\frac{[S]}{[X]}\right)\left(\frac{D_x}{D_s}\right) \quad (3)$$

[S] is the concentration of monomer probe, and [X] is the concentration of the RNA sample.

2.4. Fluorescence lifetime measurements

Fluorescence lifetimes were measured using time correlated single photon counting (TCSPC). The excitation laser system consists of a cw mode-locked Nd:YAG laser (CoherentAntares) which is frequency doubled to 532 nm and used to synchronously pump a cavity dumped dye laser. The dye laser was operated at 3.8 MHz and produced a total power of approximately 100 mW at 600 nm with a pulse width of 10 ps. The dye laser was frequency doubled in KDP to produce the UV used for excitation with an average power typically less than 1 mW. The UV was directed to the sample cuvette and fluorescence collected at right angles with f/1 optics and then focused with an f/7 lens onto the entrance slit of a 0.1 m monochrometer (ISA, Inc., Model DH-10). A polarizer in the detection path was set to the magic angle to eliminate any anisotropy contributions that might have been a particular concern for the RNA samples. The detector was a microchannel plate photomultiplier (Hamamatsu Inc. R1564U-06). The signal was collected in the single photon counting mode and captured by a PC based multi-channel analyzer (FAST ComTec, GmbH). Typical fluorescence decay curves consisted of 8192 time channels over a total range of 50 ns with the counts in the peak channel accumulated to a total of 20,000. The fluorescence decay curves were fit using the commercially available program Globals Unlimited [13].

It was found that a four exponential decay model was required to adequately fit the fluorescence decay data. The criteria for a good fit were the χ^2 values and a visual inspection of the residual. Using a 3 component, or less, exponential fit led to significantly worse values of χ^2 and resulted in the residual having a noticeable systematic variation. The fluorescence decays were thus represented by the following function.

$$I(t) = \sum_{i=1}^{4} \alpha_i e^{(-t/\tau_i)} \quad (4)$$

where $I(t)$ is the fluorescence intensity, α_i are the pre-exponentials and τ_i are the lifetimes. Total fluorescence intensity is $I = \sum_{i=1}^{4} \alpha_i \tau_i$. The percentage of each component contributing to the fluorescence intensity is $I_i\% = (\alpha_i \tau_i)/I$. The intensity weighted mean lifetime is [7]:

$$\langle \tau_m \rangle = \frac{\sum_{i=1}^{4} \alpha_i \tau_i^2}{\sum_{i-1}^{4} \alpha_i \tau_i}. \quad (5)$$

The species-concentration weighted mean lifetime is [7]:

$$\langle \tau \rangle = \frac{\sum_{i-1}^{4} \alpha_i \tau_i}{\sum_{i=1}^{4} \alpha_i} \quad (6)$$

3. Results

3.1. Fluorescence of A-3CPh and A-4CPh monomers

The UV absorption, excitation, and emission spectra of A-3CPh and A-4CPh monomers in water are shown in Fig. 1. The fluorescence properties of both probes are reported in Table 1. Both A-3CPh and A-4CPh monomers have UV absorption maxima at 215 nm with a second strong absorption peak at 262 nm (Fig. 1b). The emission spectrum of A-3CPh exhibits two distinct peaks,

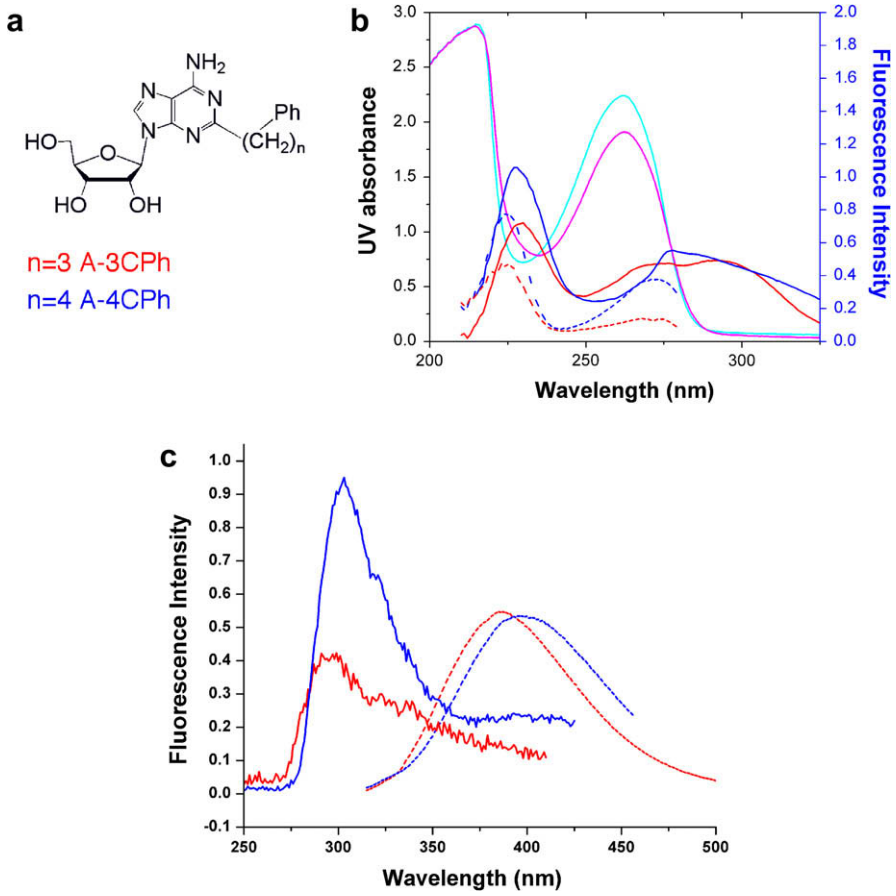

Fig. 1. (a) Diagram of the free nucleosides, A-3CPh and A-4CPh. (b) UV absorbance spectra of 200 μM A-3CPh (magenta solid line) and 230 μM A-4CPh (cyan solid line), excitation spectra for 200 μM A-3CPh emission at 387 nm (red solid line) and 10 μM A-3CPh emission at 300 nm (red dashed line), and excitation spectra for 230 μM A-4CPh emission at 397 nm (blue solid line) and 11.5 μM A-4CPh emission at 300 nm (blue dashed line). (c) Emission spectra for 10 μM A-3CPh excited at 220 nm (red solid line) and 200 μM A-3CPh excited at 300 nm (red dashed line) and emission spectra for 11.5 μM A-4CPh excited at 224 nm (blue solid line) and 230 μM A-4CPh excited at 300 nm (blue dashed line). All spectra were acquired in water. (For interpretation of the references in color in this figure legend, the reader is referred to the web version of this article.)

Table 1
The relative quantum yields (Q_{rel}) and lifetimes (τ) of the two adenosine analogs, A-3CPh and A-4CPh

	Ex_{max} (nm)	Em_{max} (nm)	Q_{rel}[a]	τ_i (ns)[b]	α_i	I% (%)	τ_m (ns)	$<\tau>$(ns)
A-3CPh	228	385	0.011 ± 0.002	τ_1 = 0.20	α_1 = 0.33	2	6.22	3.15
	274			τ_2 = 1.33	α_2 = 0.18	8		
	292			τ_3 = 5.07	α_3 = 0.43	69		
	—			τ_4 = 12.65	α_4 = 0.05	22		
A-4CPh	225	396	0.007 ± 0.001	τ_1 = 0.43	α_1 = 0.23	2	7.13	4.65
	278			τ_2 = 2.17	α_2 = 0.18	9		
	—			τ_3 = 6.20	α_3 = 0.51	68		
	—			τ_4 = 12.64	α_4 = 0.08	22		

[a] The excitation wavelength of the quantum yield measurement is 300 nm.
[b] The emission wavelength of the lifetime measurement is 410 nm.

one at 295 nm and one at 387 nm (Fig. 1c). When detecting at 387 nm, A-3CPh has an excitation maximum at 228 nm, but also exhibits significant peaks at 274 and 292 nm (Fig. 1b). Detection at 300 nm yields similar peaks in the excitation spectrum, however, the excitation peak at 291 becomes obscured due to scattered light. The emission spectra for A-4CPh exhibit similar emission peaks to A-3CPh at 303 and 396 nm (Fig. 1c). The excitation spectra for A-4CPh are quite similar to those of A-3CPh except that the two peaks to the red (274 and 292 nm in A-3CPh) appear more as a peak at 278 nm with a shoulder to the red suggesting a second overlapping peak (Fig. 1b).

The quantum yield for fluorescence was measured for each probe by comparison to standard quinine sulfate solutions as described above. The excitation wavelength used was 300 nm, which corresponds to absorption near the peak of the redder band in the fluorescence excitation band. This wavelength was chosen because it minimized the effect of competing absorption from the other bases in the RNA samples, which will be presented below. The resulting quantum yields of A-3CPh and A-4CPh are 0.011 and 0.007, respectively, as summarized in Table 1.

The fluorescence lifetimes of the probes are also reported in Table 1. The data is fit well to a four component exponential decay model with the decay times and pre-exponential factors listed. The χ^2 values for the fits were 1.1–1.3. The mean lifetime [$<\tau_m>$ – Eq. (5)] of A-3CPh is 6.22 ns, and the mean lifetime of A-4CPh is 7.13 ns.

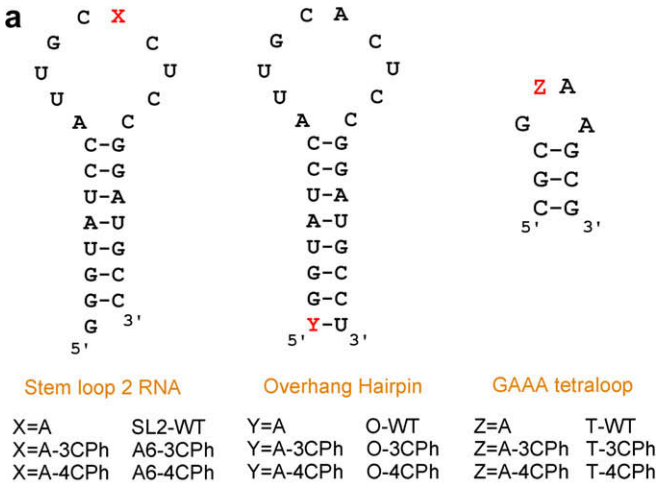

Fig. 2. (a) Secondary structure representations of the synthetic RNA hairpins and tetraloop. (b) Crystal structure of GAAA-tetraloop [34]. The first adenosine in the loop is in magenta, while the other two adenosines in the loop are in green. The three-step-stacking between the three adenosines in the loop is shown. (For interpretation of the references in color in this figure legend, the reader is referred to the web version of this article.)

3.2. RNA hairpins used in this study

Three types of RNA hairpins, designated stem loop 2 RNA, overhang hairpin, and GAAA-tetraloop (Fig. 2), were chosen to investigate the fluorescence of the base analogs in different structural environments and to probe the effect of the base analogs on the stability of different RNA structures. The stem loop 2 RNA and the overhang hairpin were based on the U1snRNA stem loop 2 RNA (SL2) that was used in the protein binding studies described previously [11]. Wild type stem loop 2 (SL2-WT) contains adenosine at the sixth position of the loop. To investigate the base analogs in a flexible, non-base paired RNA sequence, A6 was replaced by the two fluorescence probes, A-3CPh and A-4CPh, in the A6-3CPh and A6-4CPh RNAs, respectively. The second type of RNA hairpin, the overhang stem loop RNA, has the same sequence as the U1 snRNA stem loop 2 RNA except for the first base pair of the stem. Instead of a dangling G at the 5′end, the wild type overhang stem loop (O-WT) contains an A–U base pair at the end of the stem. When the 5′ adenosine of overhang stem loop is replaced by A-3CPh (O-3CPh) or A-4CPh (O-4CPh), the purine group of the modified adenosine can form a base pair with the 3′ uracil, and leave the tethered phenyl ring dangling at the 5′ end. The overhang hairpin was used to investigate the ability of the phenyl ring to affect the stability of the helix by packing against the end of the helix.

The third type of hairpin is an RNA tetraloop (four nucleotides in the loop). In solution structures [14–16] and an X-ray structure [17] of GAAA-tetraloops, the guanosine at the first position (G_1) and the adenosine at the fourth position (A_4) in the loop form non-Watson–Crick hydrogen bonds, and the adenosines at the second (A_2) and the third position (A_3) of the loop form a three-step-stacking interaction with A_4 (Fig. 2b). The hydrogen bonding and stacking interactions formed in the loop region stabilize the GNRA tetraloop [18]. The two modified adenosines, A-3CPh and A-4CPh, were incorporated into the A2 position so that the phenyl ring would be able to associate with the stacking adenines, which could alter the stability of the tetraloop and the fluorescent characteristics of the fluorescent probes. The tetraloop sequence used in this study was adapted from a paper reported by Worner et al. [19].

The CD and UV spectra of the stem loop 2 hairpin, the overhang hairpin, and GAAA-tetraloop RNAs containing A-3CPh and A-4CPh recorded from 200 to 300 nm were identical to those of the respective wild type RNAs. In order to determine the effect of the two probes on the stabilities of the RNAs, the thermal stabilities of RNA hairpins were measured using UV spectroscopy. The melting temperatures (T_m) of RNAs were determined assuming a two-state model. Two transitions were observed for the stem loop 2 and overhang RNAs, a pre-melt transition and the melting transition. A pre-melt transition has been reported previously for stem loop 2 RNA [20]. An exception to this behavior was O-3CPh for which it was difficult to distinguish the two transitions, and the melting curves were dominated by the pre-melt transition. Only one transition was observed in the melting curves of the three tetraloop RNAs. The T_m values for the three types of RNAs containing the probes compared to the values for the wild type RNAs are listed in Table 2. Although there is some deviation from wild type values for the RNAs containing A-3CPh and A-4CPh, there is no clear trend of increased or decreased T_m values upon incorporation of A-3CPh or A-4CPh into the RNA sequences.

3.3. Fluorescence of RNAs containing A-3CPh and A-4CPh

When the probes are incorporated in the various RNA sequences the absorption spectrum is dominated by contributions from bases other than the probe. For this reason the focus was on the absorption feature at 300 nm, which is significantly less influenced by the RNA, yet provides a sensitive fluorescence probe. Incorporating the A-3CPh fluorophore into RNA hairpins causes a red shift of the emission wavelength maximum compared to the free probes, except for the emission maximum of T-4CPh, which is unchanged compared to the free probe (Fig. 3 and Table 3). Overall the peak shifts are quite small.

Incorporation of A-3CPh and A-4CPh into RNA hairpins substantially enhanced fluorescence. In A6-3CPh and A6-4CPh RNAs, the fluorophores were placed in the middle of a 10-base loop, and the relative quantum yields of both probes were enhanced com-

Table 2
Melting temperature (T_m) of RNA hairpins measured by UV absorption spectroscopy

	Pre-melt transition		Melting transition	
	260 nm	280 nm	260 nm	280 nm
SL2-WT	50 ± 1	50.4 ± 0.4	62 ± 1	62 ± 1
SL2-A6-3CPh	49 ± 2	49 ± 1	64.3 ± 0.3	64.5 ± 0.3
SL2-A6-4CPh	49 ± 1	52 ± 5	64.4 ± 0.1	64.8 ± 0.4
O-WT	49 ± 5	47 ± 4	68.5 ± 0.7	69 ± 1
O-3CPh	45 ± 3	49 ± 6	—	—
O-4CPh	45 ± 1	45 ± 3	68.8 ± 0.3	69.0 ± 0.3
T-WT	—	—	61.9 ± 0.3	62.9 ± 0.6
T-3CPh	—	—	64.4 ± 0.5	60.8 ± 0.2
T-4CPh	—	—	59.1 ± 0.2	60.5 ± 0.4

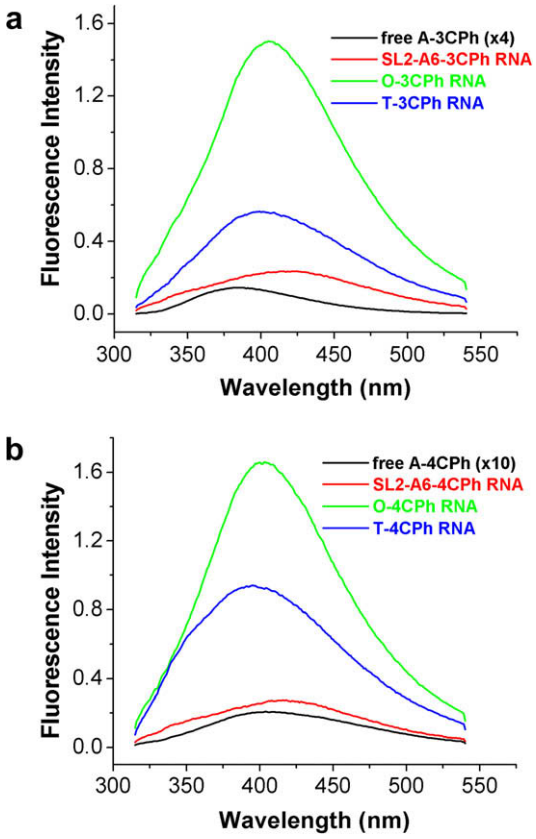

Fig. 3. Fluorescence emission spectra of RNAs containing A-3CPh and A-4CPh. The excitation wavelength was 300 nm. (a) Overlay of emission spectra of the 200 μM free A-3CPh (black, the intensity is increased 4-fold), 5 μM SL2-A6-3CPh RNA (red), 10 μM O-3CPh RNA (green), and 8 μM T-3CPh (blue). (b) Overlay of emission spectra of the 230 μM free A-4CPh probe (black, the intensity is increased 10-fold), 5 μM SL2-A6-4CPh RNA (red), 5 μM O-4CPh RNA (green), and 7.5 μM T-4CPh RNA (blue). (For interpretation of the references in color in this figure legend, the reader is referred to the web version of this article.)

pared to the free probes by 20- and 35-fold, respectively. Placing the probes at the 5′ end of stem region of the overhang RNA enhanced the quantum yields of A-3CPH and A-4CPh by 29 and 82-fold, respectively, compared to the free probe. Only 15- and 11-fold enhancements of quantum yields were observed when the probes were incorporated into the GAAA-tetraloop. The quantum yields of the probes in the RNA are calculated relative to the quantum yields of the free probes as described in Section 2. These calculations assume that the molar extinction coefficient (ε) of the free probe is similar to that of the probe in the RNA. Although it is likely that there is some change in ε upon incorporation of the probes into RNA, an increase of 11- to 82-fold of ε would result in a noticeable change in the UV spectrum. Thus, the changes in calculated quantum yield are not likely to be due to differences of ε between the free probes and the probes in the RNA.

For both probes, incorporation into RNAs reduced their mean lifetime compared to that of the monomer. The mean lifetime of A-3CPh and A-4CPh became 27% and 31% shorter when they were incorporated into stem loop 2 RNA. Incorporating the probes into overhang RNA reduced the mean lifetime of A-3CPh by 40% and that of A-4CPh by 37%. The mean lifetimes of A-3CPh and A-4CPh in tetraloop RNAs are 23% and 40% shorter than those of free probes. For the free probes, the long lifetime component is dominant. In the RNA samples the shorter lifetime components are more significant. Table 3 contains a complete summary of the quantum yield and lifetime data for the RNA samples.

4. Discussion

The fluorescence probes, A-3CPh and A-4CPh, do not alter the secondary structures of RNAs. For all three types of RNAs used in this study, the CD spectra of the RNAs containing A-3CPh and A-4CPh are identical to those of the respective wild type RNAs. Incorporation of the modified bases, A-3CPh and A-4CPh, into the RNA sequences did not alter their stability significantly. The only exception was O-3CPh for which the contributions of the pre-melting and melting transitions changed relative to the wild type RNA.

Table 3
Fluorescence properties of the oligonucleotides containing the two adenosine analogs, A-3CPh and A-4CPh

	Em_{max} (nm)	Q_{rel}[a]	Enhancement	τ_i (ns)[b]	α_i	I% (%)	τ_m (ns)	$<\tau>$ (ns)
A-3CPh	385	0.01	1	—	—	—	6.25	3.15
A6-3CPh	422	0.22 ± 0.04	20.1 ± 3.7	τ_1 = 0.15	α_1 = 0.57	8	4.57	1.16
				τ_2 = 1.07	α_2 = 0.26	24		
				τ_3 = 3.39	α_3 = 0.14	43		
				τ_4 = 10.59	α_4 = 0.03	25		
O-3CPh	405	0.32 ± 0.04	29.4 ± 4.0	τ_1 = 0.16	α_1 = 0.50	7	3.74	1.25
				τ_2 = 1.04	α_2 = 0.27	23		
				τ_3 = 2.81	α_3 = 0.20	46		
				τ_4 = 8.40	α_4 = 0.04	25		
T-3CPh	399	0.17 ± 0.02	15.0 ± 1.5	τ_1 = 0.17	α_1 = 0.53	7	4.78	1.41
				τ_2 = 1.17	α_2 = 0.27	23		
				τ_3 = 3.96	α_3 = 0.17	49		
				τ_4 = 11.12	α_4 = 0.03	22		
A-4CPh	396	0.007	—	—	—	—	7.13	4.65
A6-4CPh	416	0.25 ± 0.01	35.0 ± 0.9	τ_1 = 0.20	α_1 = 0.56	8	4.90	1.44
				τ_2 = 1.25	α_2 = 0.25	21		
				τ_3 = 4.06	α_3 = 0.17	49		
				τ_4 = 11.45	α_4 = 0.03	21		
O-4CPh	403	0.57 ± 0.02	82.0 ± 3.2	τ_1 = 0.15	α_1 = 0.52	6	4.50	1.30
				τ_2 = 0.95	α_2 = 0.23	17		
				τ_3 = 2.77	α_3 = 0.20	44		
				τ_4 = 9.08	α_4 = 0.05	34		
T-4CPh	395	0.08 ± 0.002	11.5 ± 0.3	τ_1 = 0.18	α_1 = 0.56	8	4.25	1.25
				τ_2 = 1.27	α_2 = 0.27	27		
				τ_3 = 3.44	α_3 = 0.15	40		
				τ_4 = 10.26	α_4 = 0.03	24		

[a] The excitation wavelength of the quantum yield measurement is 300 nm.
[b] The emission wavelength of the lifetime measurement is 410 nm.

Thus, the incorporation of the probes into these three RNA sequences did not significantly change the structure or stability of the RNAs.

The fluorescence behavior of these probe molecules is quite complex, particularly considering the substantial change in quantum yield when incorporated into the various RNA oligomers. One of the first things to note is the presence of two distinct emission bands, one at ~300 nm and the other at ~400 nm. According to Kasha's rule one expects fluorescence to arise from the lowest excited state of the correct multiplicity, in this case a singlet state. The dual emission can be explained by the presence of two tethered chromophores. The emission at 300 nm can be ascribed to resonant fluorescence of the phenyl moiety red-shifted somewhat from that of benzene in aqueous solution [21]. Adenosine is the model for the second chromophore and it has an absorption peak at 259 nm with a molar extinction coefficient of 15,400 M^{-1} cm^{-1} [22]. However, with regard to the emission behavior adenosine is essentially non-fluorescent with a quantum yield of 2.6×10^{-4} [23].

The probe molecule emission band at ~400 nm is more difficult to account for. Neither adenosine nor phenyl has emission features in this region and so it must be a property of the entire molecule. An obvious possibility is that an impurity is responsible for this emission band. We consider this unlikely for several reasons. First, the free probes were rigorously purified and characterized by NMR and mass spectrometry. Second, similar results were obtained from two independent syntheses of the free probes. Third, the fluorescence properties of the free probe and the RNA are similar, except for the relative quantum yields. Thus, an impurity would have had to first been carried through the three-step synthesis to form the phosphoramidite. Then, this impurity would either have to have been incorporated into all of the RNAs or been carried along through the solid phase synthesis and purification of the RNAs by gel electrophoresis. Buffer solutions were routinely checked for contamination and showed no fluorescence consistent with the probe molecules.

There are two likely possibilities for the emission at 400 nm. First is an exciplex formed intramolecularly between the phenyl and adenosine. Several observations make this unlikely. First, the emission at 300 nm and 400 nm are both seen to increase upon incorporation into RNA. Clearly formation of an exciplex would lead to a loss of fluorescence from the phenyl moiety and emission intensity at these wavelengths would be anti-correlated. Second, there are many examples in the literature of exciplexes formed between aromatic groups with a C_3 linker but not with a C_4 linker (the so called Hirayama's $n = 3$ rule [24]). For the probes studied here the behavior of the $n = 3$ and $n = 4$ linked species are quite similar. Finally, incorporation of the probes in RNA would appear to block access of the adenosine π system from the phenyl thus, inhibiting the formation of an exciplex, not enhancing it as would be required to explain the fluorescence increase.

A second possible explanation for the emission at 400 nm is a modification of the electronic structure of adenosine that leads to an increase in quantum yield and a red-shifted spectrum. The emission at 400 nm is thus ascribed to emission from an excited state of the substituted adenosine. There is an extensive literature documenting the photophysics of adenosine [25–28]. In particular there have been a number of theoretical treatments attempting to understand the details of the excited state behavior [25,26,28–32] The emission behavior of adenosine (very low quantum yield) and its sensitivity to substitution have been described in terms of the relative energetics of the π–π^* and n–π^* excited states [25,26,28,31]. More recently it has been proposed that the location of a conical intersection, which gives access to the ground state, S_0, is responsible for the non-radiative behavior [28,29,32]. For the probes considered here the 400 nm emission cannot be due to an intermolecular interaction with neighboring bases in RNA, such as charge transfer or exciplex formation, since the free probe fluorescence spectrum and lifetime are qualitatively quite similar to the probes in RNA, just much weaker.

Independent of these two models there is strong evidence that the excited state species emitting at 400 nm originates from a subpopulation of the probe molecules. The first observation supporting this is that the fluorescence lifetime is very similar in the monomer and the RNA samples even though the quantum yield increases by a factor of 11–82 depending on which RNA is being considered. Typically there is a linear relationship between the quantum yield, Φ, and the observed lifetime, τ_{obs}. The lifetimes of probes incorporated in RNA are quite similar to those observed in the free probes (in fact slightly shorter) even though the quantum yields of the free probe are dramatically lower. The only obvious way to explain this discrepancy between lifetime and quantum yield is to invoke significant static quenching in the free probe molecules. Static quenching arises when interactions in the ground state of the molecule leads to changes in the electronic structure such that absorption is significantly less, or more commonly, the excited state reached upon absorption is non-fluorescent.

The static quenching component is likely to originate from specific molecular conformations that are part of an equilibrium distribution of structures. One could imagine structures with specific orientations of the phenyl and adenosine moieties that lead to rapid excited state quenching. It is well known, for example in tryptophan fluorescence, that different structures can have vastly different excited state lifetimes [1]. Perhaps a closer example is the quenching which occurs in the flavin adenine dinucleotide (FAD) as reported by van der Berg et al. [33]. In that case, the strong fluorescence of the isoalloxazine ring is quenched by proximity of the adenine ring. The specific value of the quantum yield was ascribed to the ratio of closed quenching structures to open non-quenched structures. It was estimated that 80% or more of the molecules were in the quenched form. The dramatic change in quantum yield between the free probes and those incorporated in RNA is then viewed as consequence of the change in the equilibrium distribution of structures. The similarity of the emission spectra and lifetimes of the free probes and RNA samples suggests that the emitting species is quite similar in both cases, it is just that a significant change has occurred between the distribution of emitting and non-emitting structures.

The second piece of evidence supporting different sub-populations is the displacement between the absorption spectrum peak at 267 nm and the fluorescence excitation peaks, which are significantly red-shifted. As seen in Fig. 1, A-3CPh has a fluorescence excitation peak at 292 nm and A-4CPh has a peak at 278 nm with an additional shoulder further to the red. This is consistent with a minor molecular conformation that contributes proportionally to the absorption spectrum but disproportionately to the excitation spectrum because it has a dramatically larger quantum yield than the major conformations present. The emission properties of protonated adenine and adenosine cations have been shown to exhibit similar behavior [27]. In this case, the emission of the protonated adenine was found to be due to the highly fluorescent but minor tautomer protonated at both the 7 and 9 positions. In that case the fluorescence excitation spectrum was also red-shifted from the absorption.

5. Conclusion

In summary, A-3CPh and A-4CPh are fluorescent nucleotide base analogs that can be selectively incorporated into an oligonucleotide through a normal phosphodiester linkage. The presence of all of the hydrogen bond donors and acceptors of the adenosine allows the probes to participate in hydrogen bonding interactions

involving adenosine within RNA structures and RNA–protein complexes. Although they are not highly fluorescent as monomers, the quantum yields of the probes are significantly enhanced upon incorporation into single-stranded RNA. As a result, the quantum yields of these probes in RNA are similar to those of other commonly used fluorescent base analogs. Incorporating these probes into RNA does not globally change the structure and stability of the RNAs investigated here. This is consistent with previous investigations in which we found that these probes only modestly destabilize the U1A-SL2 RNA complex when substituted for an important adenine in the binding interface [11]. Thus, these probes may be useful for providing information about events occurring close to the modification site.

Acknowledgments

Funding was provided by the NIH to AMB, GM-56857. Y.Z. was supported by a NIH Training Grant in Molecular Biophysics (GM-08271).

References

[1] J.R. Lakowicz, Principles of Fluorescence Spectroscopy, second ed., Kluwer Academic/Plenum, New York, 1999.
[2] C.R. Cremo, Fluorescence nucleotides: synthesis and characterization, in: Biophotonics, Pt A. vol. 360, 2003, pp. 128–177.
[3] M.J. Rist, J.P. Marino, Curr .Org. Chem. 6 (2002) 775–793.
[4] N.J. Leonard, G.L. Tolman, Ann. NY Acad. Sci. 255 (1975) 43–58.
[5] J.N. Wilson, E.T. Kool, Org. Biomol. Chem. 4 (2006) 4264–4265.
[6] N.G. Walter, D.A. Harris, M.J.B. Pereira, D. Rueda, Biopolymers 61 (2002) 224–241.
[7] M.E. Hawkins, W. Pfleiderer, F.M. Balis, D. Porter, J.R. Knutson, Anal. Biochem. 244 (1997) 86–95.
[8] S.G. Srivatsan, Y. Tor, J. Am. Chem. Soc. 129 (2006) 2044–2053.
[9] Y. Tor, S. Del Valle, D. Jaramillo, S.G. Srivatsan, A. Rios, H. Weizman, Tetrahedron 63 (2007) 3608–3614.
[10] R.A. Tinsley, N.G. Walter, RNA 12 (2006) 522–529.
[11] Y. Zhao, A.M. Baranger, J. Am. Chem. Soc. 125 (2003) 2480–2488.
[12] J.N. Demas, G.A. Crosby, J. Phys. Chem. 75 (1971) 991–1024.
[13] J.M. Beechem, E. Gratton, Fluorescence spectroscopy data analysis environment a second generation global analysis program, in: J. Lakowicz (Ed.), Time-Resolved Laser Spectroscopy in Biochemistry, vol. 909, 1988, pp. 77–81.
[14] F.M. Jucker, H.A. Heus, P.F. Yip, E.H.M. Moors, A. Pardi, J. Mol. Biol. 264 (1996) 968–980.
[15] G.R. Zimmermann, R.D. Jenison, C.L. Wick, J.P. Simorre, A. Pardi, Nat. Struct. Biol. 4 (1997) 644–649.
[16] S. Rüdisser, I. Tinoco, J. Mol. Biol. 295 (2000) 1211–1223.
[17] H.W. Pley, K.M. Flaherty, D.B. McKay, Nature 372 (1994) 68–74.
[18] V.P. Antao, S.Y. Lai, I. Tinoco, Nucleic Acids Res. 19 (1991) 5901–5905.
[19] K. Wörner, T. Strube, J.W. Engels, Helv. Chem. Acta 82 (1999) 2094–2104.
[20] K.B. Hall, Biochemistry 33 (1994) 10076–10088.
[21] F.P. Schwarz, S.P. Wasik, Anal. Chem. 48 (1976) 524–528.
[22] M. Dworkin, K.H. Keller, J. Biol. Chem. 252 (1977) 864–865.
[23] M. Daniels, W. Hauswirth, Science 171 (1971) 675–677.
[24] F. Hirayam, J. Chem. Phys. 42 (1965) 3163.
[25] E.C. Lim, J. Phys. Chem. 90 (1986) 6770–6777.
[26] C.E. Crespo-Hernandez, B. Cohen, P.M. Hare, B. Kohler, Chem. Rev. 104 (2004) 1977–2019.
[27] W.B. Knighton, G.O. Giskaas, P.R. Callis, J. Phys. Chem. 86 (1982) 49–55.
[28] C.M. Mariana, J. Chem. Phys. 122 (2005) 104314.
[29] L. Serramo-Andres, M. Merchan, A.C. Borin, Proc. Natl. Acad. Sci. 103 (2006) 8692–8696.
[30] A. Broo, J. Phys. Chem. A 102 (1998) 526–531.
[31] B. Mennucci, A. Toniolo, J. Tomasi, J. Phys. Chem. A 105 (2001) 4749–4757.
[32] S.B. Nielson, T.I. Solling, Chem. Phys. Chem. 6 (2005) 1276–1281.
[33] P.A.W. van den Berg, K.A. Feenstra, A.E. Mark, H.J.C. Berendsen, A.J.W.G. Visser, J. Phys. Chem. B 106 (2002) 8858–8869.
[34] H.W. Pley, K.M. Flaherty, D.B. Mckay, Nature 372 (1994) 111–113.